

Interpretable Signal Analysis with Knockoffs Enhances Classification of Bacterial Raman Spectra

Charmaine Chia, Matteo Sesia, Chi-Sing Ho, Stefanie S. Jeffrey, Jennifer Dionne, Emmanuel Candès, and Roger T. Howe

Abstract—Interpretability is important for many applications of machine learning to signal data, covering aspects such as how well a model fits the data, how accurately explanations are drawn from it, and how well these can be understood by people. Feature extraction and selection can improve model interpretability by identifying structures in the data that are both informative and intuitively meaningful. To this end, we propose a signal classification framework that combines feature extraction with feature selection using the knockoff filter, a method which provides guarantees on the false discovery rate (FDR) amongst selected features. We apply this to a dataset of Raman spectroscopy measurements from bacterial samples. Using a wavelet-based feature representation of the data and a logistic regression classifier, our framework achieves significantly higher predictive accuracy compared to using the original features as input. Benchmarking was also done with features obtained through principal components analysis, as well as the original features input into a neural network-based classifier. Our proposed framework achieved better predictive performance at the former task and comparable performance at the latter task, while offering the advantage of a more compact and human-interpretable set of features.

Index Terms—Signal processing, wavelet transform, knockoff filter, Raman spectroscopy, classification, interpretability, predictive accuracy, descriptive accuracy, relevancy

I. INTRODUCTION

SIGNAL data comes in a wealth of different forms, from biomedical and environmental sensor measurements, to spectrograms, audio and image data, and financial time series. These consist of sequential measurements of an observable along an independent variable axis, and they often differ from structured data in that the meaning of each measured variable is not as distinctively and intuitively definable. To perform predictions from signal data, we need to apply signal processing and machine learning (ML) techniques to extract features that contain information about the signal and its sources. While predictive accuracy is usually prioritized, the ability to interpret what an ML model has learned is gaining increasing attention [1]. Interpretability is crucial when a model’s predictions can have serious consequences, as in applications involving healthcare, transport, defense, or finance, and it can also be

useful for model debugging, increasing social acceptance, and auditing predictions to account for issues like fairness. Furthermore, when the signal source itself is not well understood, model interpretations can yield insights into the behavior of the source and potentially allow inferences to be drawn and then validated through additional experiments.

The PDR framework recently introduced by Murdoch *et al* proposes three metrics for evaluating model interpretations: 1) Predictive accuracy (how well the model fits the underlying data), 2) Descriptive accuracy (the fidelity of the interpretation in describing relationships learned by the model), and 3) Relevancy (how useful and comprehensible the interpretation is to the target audience) [2]. Simpler ML models, such as linear or logistic regression, decision trees, and Naïve Bayes, offer superior interpretability, though often at the expense of predictive accuracy. On the other hand, more complex models such as neural networks are better at capturing non-linear and hierarchical relationships in the data, achieving unprecedented predictive performance in fields like computer vision and natural language processing [4,5]. “Feature extraction” here is done automatically by backpropagation to tune weights in a neural network of predefined architecture. Unfortunately, in addition to the high computational overhead for training such models, their complexity and “black box” nature make these features difficult to access and interpret intuitively. Various *post-hoc* interpretation methods have been developed to improve descriptive accuracy; for example, saliency methods help visualize the activation of individual input features or weights [7], while Feature Attribution methods like LIME (Local Interpretable Model-agnostic Explanations) and SHapley Additive exPlanations (SHAP) measure the explanatory power of each feature on the predictions of the black box model, by fitting surrogate models on permuted subsets of the input data [3,8]. Nonetheless, these methods have their own limitations: some instability and ambiguity in the neighborhood of inputs to perturb for LIME, as well as high computational cost for SHAP. Ultimately, relevancy often plays a key role in determining which model to use based on the desired trade-off between predictive and descriptive accuracy.

C. Chia (email: charmaine@aetherbio.com) was in the Department of Electrical Engineering at Stanford University, Stanford, CA 94305, coadvised by R. T. Howe and S. S. Jeffrey. She is now with Aether Biomachines, Menlo Park, CA 94025 USA.

M. Sesia (email: msesia@stanford.edu) is in the Department of Statistics at Stanford University, and is advised by E. Candès.

C-S. Ho was in the Department of Applied Physics at Stanford University, advised by J. Dionne.

With regard to relevancy, studies from the social sciences reported that people tend to favor explanations that are short (selecting a few key causes), contrast one instance with another of a different outcome, and which highlight abnormal causes [9]. In other words, we seek to understand which explanatory features are important, and how these affect the outcome. Data scientists often pursue these goals through feature selection, in addition to feature extraction, to ensure that their predictions are based on relevant, non-redundant predictors. For example, researchers may want to identify a smaller set of genetic variants out of thousands of possibilities that are linked to cancer susceptibility, or identify which of a myriad of possible specific morphological and textural extractable from brain electroencephalogram (EEG) signals can diagnose epilepsy [10]. In practice, when the number of potential predictors is large, some selected features will likely be false discoveries: false positives in which we wrongly reject the null hypothesis when the feature has no effect on the outcome. In this case, the null hypothesis for a given feature would be that it is not predictive given the others, and contains no additional information on the outcome of interest (see Appendix). False discoveries can lead to erroneous communications, prescriptions, and policy decisions. Controlling the false discovery rate (FDR), the expected ratio of the number of false discoveries to the total number of discoveries, is thus an important goal when performing feature selection to obtain relevant and human-friendly interpretations of ML models.

Toward this end, Barber and Candès developed the Knockoff Filter, a feature selection technique that provides a mathematical guarantee for the maximum FDR amongst selected features in a linear regression setting [11]. Candès, Fan, Janson, and Lv later extended this to a general non-parametric regression setting [12], which includes the multi-class classification problem considered in this paper. The idea of [12] is to generate a set of *knockoff* features that mimic the correlation structure of the original features, but are conditionally independent of the response given the original features. The knockoffs can then be used as a negative control when performing feature selection, by comparing some measure of feature importance between corresponding original and knockoff features (see Appendix).

The knockoff framework has attracted significant interest due to its strong FDR control while preserving predictive power. However, most of the application-oriented literature has so far focused on structured biomedical data in the form of genetic data [13-16] and demographic/behavioral cancer biomarkers [17]. In these cases, the features are well-defined a priori, for example in the form of single nucleotide polymorphisms (SNP's) in the genome. Only a few extensions to unstructured signal-type data have been reported, namely on a dataset of computed tomography (CT) images for lung cancer diagnosis [18], functional magnetic resonance (fMRI) images for Alzheimer's studies [19], and time series for economic forecasting [20]. This relatively unexplored area provides a valuable use case for the knockoffs approach to controlled feature selection, especially for modalities of sensor signals that

have not been well studied, or for which the raw features may not be very informative.

To deal with this, we introduce a framework that combines feature extraction with knockoff filter-based feature selection for interpretable signal analysis, and demonstrate its utility by applying it to fast Raman spectroscopy measurements of common bacteria samples from the Stanford Hospital [21]. Here, the problem is to classify each sample by type of bacteria. Based on the interaction of laser light with the vibrations of molecular bonds in the sample, Raman spectroscopy measures the energy shifts of incident photons due to inelastic scattering, thus giving an optical fingerprint of the sample. The same principle applies to the fast Raman measurements, but because of the much shorter measurement times, those spectra are noisier and the features less identifiable. This dataset was recently found to be successful for predicting outcomes like bacterial strain and antibiotic susceptibility by using a convolutional neural network (CNN)-based analysis [21]. The results are promising for rapid and culture-free pathogen identification, which could advance the treatment of bacterial infections and sepsis. At the same time, the high stakes of these medical decisions call for a more interpretable form of modeling which could, in parallel, shed light on features of predictive importance that potentially correspond to distinguishing chemical features in the dataset. This is what our framework enables as a general wrapper beginning with a feature extraction step that transforms the signal data into a better representation to input into the ML model. Using a simple multinomial logistic regression model for prediction, we show that applying the framework reduces overfitting and improves the predictive accuracy, yielding comparable performance to the CNN. It also results in a more compact and interpretable representation of the data, improving the relevancy of the analysis.

In the following sections, we describe the dataset to which we apply our framework, outline methods for feature extraction that can be employed on signal data, motivate the choice of a wavelet-based representation for our fast Raman spectroscopy signals, and describe the knockoffs generation and classification procedures. Finally, we then discuss the results of applying the framework to the Raman dataset.

II. DATASET

The raw signal data (X) used to test our proposed framework was acquired by the J. A. Dionne group in the Materials Science and Engineering Department at Stanford [21]. The dataset consists of 60,000 Raman spectra of dried monolayer bacteria and yeast samples taken with fast (one second) scans. Thirty distinct isolates were measured including multiple isolates of Gram-negative and Gram-positive bacteria, as well as *Candida* species, with 2000 spectra measured for each isolate. Most of the spectra were taken over single cells. The spectra consist of 992 measurement points in the spectral range of 381.98 to 1792.4 cm^{-1} . The measured Raman intensities were normalized to lie between a minimum value of 0 and maximum value of 1. Further details on the measurements can be found in [21]. The datasets can be found at <https://github.com/csho33/bacteria-ID>.

A wavelet-based feature representation (X') was constructed by passing each of the 60,000 Raman signals in X through a Discrete Wavelet Transform (DWT). The basis wavelet was a 24-point Coiflet with five DWT levels. The result of the transform is a set of 1105 features which represent the concatenated approximation and detail coefficients from the five-level wavelet filtering procedure.

Three sets of outcome labels Y were available for the same input dataset:

1. Isolate labels \rightarrow 30 classes
2. Empiric antibiotic treatment \rightarrow 8 classes
3. Methicillin resistance of *Staphylococcus aureus* strains \rightarrow 2 classes

To summarize, the dataset sizes are as follows:

- Raw signal dataset (X): $60,000 \times 992$
- Wavelet representation dataset (X'): $60,000 \times 1105$
- Outcome labels (Y): $60,000 \times 1$ except for the 3rd set of labels, which apply only to *Staphylococcus aureus* strains, giving a $10,000 \times 1$ outcome matrix

III. METHODS

A. Feature extraction

Feature extraction is the transformation of the original dataset into a more discriminatory representation for the prediction task. For signal data, approaches to feature extraction fall into four broad classes [4]:

1. Time/position domain methods
2. Frequency domain methods
3. Time/position–frequency domain methods
4. Signal decomposition and sparse domain methods

where ‘time/position’ refers generally to the independent variable axis, which could be time, spatial location, voltage, *etc.*

Time/position domain methods extract characteristic properties from a window of measurement points in the signal, the simplest being the signal mean and standard deviation. Techniques like Autoregressive (AR) Modeling, Linear Predictive Coding (LPC), Cepstrum Analysis, and kernel-based methods [4] have also been used in applications such as tissue characterization, gait analysis, and compressive encoding of speech signals. **Frequency domain methods** break down signals into their spectral components, giving complementary information to time/position domain methods. The Fourier transform converts a periodic signal into a sum of sinusoidal waves. Its algorithmic variations include the Discrete Fourier Transform (DFT) and the Fast Fourier Transform (FFT), which allow for finite sampling of a digital signal, making them easier to implement on signal processing hardware. **Time/position–frequency domain methods** allow us to capture both frequency and localized time/position information in non-linear and non-stationary signals, and include the Short-Time Fourier transform (STFT) and Wavelet transform. The latter projects the signal onto a basis set of wave-like oscillations that begin and end with zero amplitude, or wavelets. It comes in two main variations: the Discrete Wavelet Transform (DWT), which uses orthogonal wavelets, and the Continuous Wavelet Transform (CWT), which returns an overcomplete representation in terms

of wavelets that are continuously shifted/scaled. The DWT trades off the fine-grained resolution of the CWT for compactness by critically sampling the signal on a dyadic grid using a filterbank which iteratively separates the low and high frequency components of the sampled signal [22]. The resulting DWT coefficients constitute a feature representation from which the original signal can be reconstructed using an Inverse Discrete Wavelet Transform (IDWT). More recently, **signal decomposition and sparse domain methods** have aimed at finding sparse representations in terms of basis sets that are *empirically* defined, paving the way to efficient real-time signal analysis. An area of active research is Dictionary Learning, which attempts to find a sparse representation x of a signal s in the form of a linear combination of ‘atoms’ in a dictionary D , $s \approx Dx$, which are not required to be orthogonal. Convolutional dictionary learning (CDL) and sparse coding (CSC) replaces the unstructured dictionary D with a set of linear filters $\{d_m\}$ which can be shorter than the length of the signal, so that the signal is the sum of convolutions of the sparse representation with dictionary filters, that is, $s \approx \sum d_m * x_m$ [23].

For our fast Raman spectroscopy dataset, we opt for an easily implemented representation with similar dimensionality as our original signal, to highlight the impact of the feature extraction module in our generalized framework. Since Raman data are spectroscopic, with expected peak-like resonance features, a wavelet-based representation is an appropriate choice. Spectroscopic signals are traditionally analyzed by fitting Gaussian or Lagrangian peaks, thus offering an interpretive basis for our extracted features.

In general, given the array of feature extraction methods ranging from ‘handcrafted’ to fully automated, the optimal choice would depend on desired properties of the signal representation, such as robustness to artifacts, compactness, intuitiveness, and information content for prediction. In addition, relevant considerations also include the PDR tradeoffs and computational constraints. It can also be useful to consider the dynamics of the signal source and utilize it as *a priori* knowledge into feature extraction to aid in pattern identification [4].

B. Knockoff generation

Knockoffs were generated for both the original (X) and wavelet representation (X') datasets using the Model-X method [12], as implemented by the *second-order knockoff machines* in [24]. The Python code for knockoff generation has been made publicly available by the Candès group at: <https://github.com/mseasia/deepknockoffs>. We have applied this algorithm to generate knockoff features that are pairwise exchangeable with the original features in terms of their second moments. More precisely, we generate the knockoff features \tilde{X} given the original features X such that the means and covariance matrices of the augmented dataset $[X, \tilde{X}]$ match those of $[X, \tilde{X}]_{\text{swap}(S)}$, for any subset S of $\{1, \dots, p\}$, where $[X, \tilde{X}]_{\text{swap}(S)}$ indicates the pairwise swapping of all features indexed by the set S with the corresponding knockoffs. Furthermore, we simultaneously try to make each element of \tilde{X} as different as possible from the corresponding element of X .

As a result, the covariance matrices of both datasets are approximately equal to:

$$G := \begin{bmatrix} \Sigma & \Sigma - \text{diag}\{s\} \\ \Sigma - \text{diag}\{s\} & \Sigma \end{bmatrix} \quad (1)$$

where Σ is the covariance matrix of X and the vector s is maximized subject to the constraint that the matrix G be positive semi-definite [8, 26]. We refer to [24] and [12] for further details on knockoff generation. It is worth mentioning here that the method in [24] and the accompanying software used in this paper can accommodate a more general construction of knockoffs (*deep knockoffs*) that matches higher moments of $[X, \tilde{X}]$ to those of $[X, \tilde{X}]_{\text{swap}(S)}$, which leads to a more robust variable selection procedure in some situations, but appeared to make little difference in our particular case. Therefore, we focus here on second-order knockoffs for simplicity.

C. Feature selection with controlled false discovery rate via Knockoffs filtering

Following knockoffs generation, the augmented raw and wavelet representation datasets $[X \ \tilde{X}]$ and $[X' \ \tilde{X}']$ were separately fed as inputs to a classifier, which was trained on each of the three sets of Y output labels. The number of features in each model was thus twice that of the original un-augmented datasets. The classification model chosen was logistic regression with L1 (lasso) regularization [25]. For the 30-class isolate identification and 8-class antibiotic treatment classification tasks, we used a multinomial logistic regression model, which outputs a probability distribution across all the classes; the maximum probability is taken as the predicted class. For the 2-class methicillin resistance classification, (binomial) logistic regression was used. L1 regularization was added to shrink the feature coefficients towards zero, resulting in sparser models.

From the fitted coefficients output for each task ($\hat{\beta}_j(\lambda)$, $\hat{\beta}_{j+p}(\lambda)$), where λ was tuned by 10-fold cross-validation, we calculated scores for each feature W_j . To perform feature selection, the adaptive threshold T was set such that knockoffs estimate of the false discovery proportion was 10%. Therefore, by selecting only features with $W_j > T$, we seek to control the FDR at that level, that is, we expect no more than 10% of the selected features to be redundant or non-predictive. If we denote the subset of features selected by each knockoff filtering procedure with \hat{S} , the datasets of features selected from the raw signal and wavelet representation are thus $\{X_j\}_{j \in \hat{S}}$ and $\{X'_j\}_{j \in \hat{S}}$, respectively.

D. Classification

To compare the performance of the features selected using the knockoffs procedure ($\{X_j\}_{j \in \hat{S}}$, $\{X'_j\}_{j \in \hat{S}}$) against the full set of raw and wavelet features (X, X'), we trained classification models on all 12 prediction tasks arising from combination of these four input datasets and the three sets of Y output labels:

$$\begin{bmatrix} X \\ \{X_j\}_{j \in \hat{S}} \\ X' \\ \{X'_j\}_{j \in \hat{S}} \end{bmatrix} \times \begin{bmatrix} Y_{30\text{-class}} \\ Y_{8\text{-class}} \\ Y_{2\text{-class}} \end{bmatrix}$$

As before, the classification model chosen was logistic regression-based with L1 regularization. Model performance was evaluated using 5-fold cross-validation, with results reported for the test set. The classifiers were implemented using the **glmnet** package in R [26].

By comparing the results from these 12 prediction tasks, we can evaluate: (A) the effect of applying feature extraction, and (B) the effect of feature selection via the Knockoff Filter, thus allowing us to validate the contribution of each of these modules to our proposed signal handling framework.

In addition, model performance was benchmarked against classification results obtained from a CNN, SVM, and logistic regression models reported in [27]. Fig. 1 summarizes the procedures in our framework.

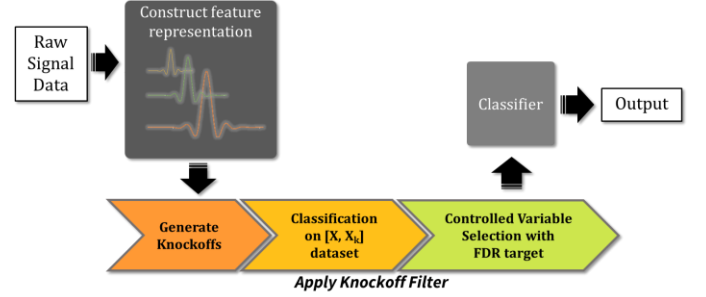


Fig. 1. Analysis framework with controlled feature selection and classification

IV. RESULTS AND DISCUSSION

Table 1 summarizes the classification errors obtained on the three prediction tasks (30, 8, and 2 classes) using each of the four input datasets: X , $\{X_j\}_{j \in \hat{S}}$, X' , $\{X'_j\}_{j \in \hat{S}}$. The rows for the knockoff-filtered datasets are highlighted in yellow and arranged below the rows for the corresponding unfiltered dataset. The knockoff-filtered datasets were obtained using knockoffs generated with the second order method previously described. The number of non-zero coefficients output refers to the number of features selected by the lasso logistic regression classifier, using the cross-validated λ value.

TABLE 1

Comparison of model performances on raw and wavelet representation datasets, before and after applying the Knockoff Filter

Input	# of classes in prediction task	# of input features	# of non-zero coeffs output	Test error (%)	Error S.D. (%)
X	30	992	457	7.4	0.3
$\{X_j\}_{j \in \hat{S}}$	30	982	454	7.3	0.2
X'	30	1105	328	6.7	0.3
$\{X'_j\}_{j \in \hat{S}}$	30	152	121	5.3	0.2
X	8	992	552	5.5	0.2
$\{X_j\}_{j \in \hat{S}}$	8	913	532	5.5	0.3
X'	8	1105	436	5.3	0.2
$\{X'_j\}_{j \in \hat{S}}$	8	103	93	4.9	0.2
X	2	992	687	7.2	0.6
$\{X_j\}_{j \in \hat{S}}$	2	551	526	6.8	0.5
X'	2	1105	239	6.1	0.7
$\{X'_j\}_{j \in \hat{S}}$	2	63	63	5.7	0.5

A. Classification performance with and without feature extraction

To examine the effect of feature extraction (in this case transforming the raw Raman signals to a wavelet representation), we compare the classification errors for input datasets X and X' (*i.e.*, the unhighlighted columns), for each of the three tasks. In each case, we observe a decrease in test error, from 7.4% to 6.7% for the 30-class task, from 5.5% to 5.3% for the 8-class task, and from 7.2% to 6.1% for the 2-class task.

TABLE 2

Comparison of model performances on raw-PCA and knockoff-filtered wavelet representation datasets with the same number of features

Input	# of classes in prediction task	# of input features	# of non-zero coeffs output	Test error (%)	Error S.D. (%)
X_{PCA152}	30	152	117	6.1	0.3
$\{X'_j\}_{j \in \hat{S}}$	30	152	121	5.3	0.2
X_{PCA103}	8	103	83	5.2	0.3
$\{X'_j\}_{j \in \hat{S}}$	8	103	93	4.9	0.2
X_{PCA63}	2	63	29	6.4	0.8
$\{X'_j\}_{j \in \hat{S}}$	2	63	63	5.7	0.5

We also performed Principal Component Analysis (PCA) on the raw signal dataset. PCA extracts directions in the matrix dataset along which the data has the most variance. The top 152, 103, and 63 components were fed as features into the lasso logistic regression model to perform the 30, 8 and 2-class predictions, respectively, and the results are shown in the unhighlighted columns of Table 2. The number of components was chosen to match the number of wavelet features in \hat{S} selected by the knockoffs procedure. Once again, the wavelet representation features yielded lower classification errors in each of the three tasks.

Together, these results suggest that the wavelet features are not only more informative than the raw signal features, but that they are also better than the equivalent number of top PCA components from the raw signal. We conclude that feature extraction can have a significant positive impact on model performance.

B. Classification performance before and after applying the Knockoff Filter

To examine the effect of applying the Knockoff Filter, we compare the classification errors for adjacent pairs of rows in Table 1 for each of the three tasks. These rows correspond to input datasets before (unhighlighted) and after (highlighted) using the knockoffs procedure to select features at an FDR target of 10%.

In general, we observe a significant improvement in classification error between X' and $\{X'_j\}_{j \in \hat{S}}$ when we apply the Knockoff Filter to the wavelet representation dataset before training the final classifier. In particular, the test error decreases from 6.7% to 5.3% for the 30-class task, from 5.3% to 4.9% for the 8-class task, and from 6.1% to 5.7% for the 2-class task. This result is notable given that the number of features input into the classifier is very much reduced — from the original 1055 wavelet coefficient features, we are left with only 152, 103, and 63 features for the respective tasks. The unfiltered model was possibly overfitting the training data and causing poorer performance on the test data, despite the fact that the L1 penalty had already significantly downsized the logistic regression model by selecting only 328, 436, and 239 features. The Knockoff Filter evidently does a better job at feature selection, giving us a more compact set of features with improved prediction accuracy, as well as an FDR guarantee.

The effect of the Knockoff Filter is less obvious when we compare the raw signal-based datasets, X and $\{X_j\}_{j \in \hat{S}}$. The knockoff-filtered dataset is only marginally downsized from the original dataset in each of the three prediction tasks, giving minimal changes in classification error. This suggests that the raw signal features are on average less informative than the wavelet representation features, and cannot be directly “sparsified” without loss of predictive power. As there are many more features that are weak predictors, the combination of which is required to achieve reasonable classification performance, the knockoffs method is less effective in filtering out these features. In contrast, the wavelet features are more informative and natural predictors, but they are redundant. Therefore, the knockoffs can sparsify them without losing predictive accuracy, and even help to improve performance by reducing overfitting.

C. Benchmarking against the performance of other classifiers

Table 3 benchmarks the performance of our proposed signal analysis framework (see Fig. 1, a wavelet-based feature extraction, knockoffs feature selection, followed by a lasso logistic regression (LLR) classifier) against that of other classifiers on the same raw Raman data. Specifically, we include the 5-fold cross-validation errors previously reported using a convolutional neural network (CNN)-based classifier,

as well as support vector machine (SVM) and logistic regression (LR)-based classifiers without regularization [27]. The input features to the SVM and LR classifiers were the top 20 PCA components of the raw signal dataset; justification for the choice of feature number is provided in [27].

TABLE 3

Benchmarking of test errors obtained with our framework to other models. Results in unhighlighted columns are quoted from [27].

Input	Classifier	# of classes in prediction task	# of input features	# of non-zero coeffs output	Test error (%)	Error S.D. (%)
X	CNN	30	992	992	6.2	0.1
X_{PCA20}	SVM	30	20	20	11.3	0.2
X'	LR	30	20	20	10.7	0.2
$\{X'_j\}_{j \in \mathcal{S}}$	LLR	30	152	121	5.3	0.2
X	CNN	8	992	992	1.0	0.1
$\{X_j\}_{j \in \mathcal{S}}$	LLR	8	103	93	4.9	0.2
X'	CNN	2	992	992	4.6	0.5
$\{X'_j\}_{j \in \mathcal{S}}$	LLR	2	63	63	5.7	0.5

Overall, our proposed framework performs significantly better than both the SVM and LR classifiers on the 30-class task, yielding almost half the prediction error. Its performance is roughly equivalent to that of the CNN, exceeding the CNN's performance on the 30-class task, while performing worse on the 8-class and 2-class prediction tasks. The poorer performance on the latter two tasks could be due to fact that the LLR classifier only learns a linear mapping from the input features to output classes, whereas the neural network allows for complex, non-linear relationships to be modelled. The CNN seems to perform especially well on the 8-class task — likely due to this being an easier task with more examples per class than the 30-class problem, and clearer distinctions between the classes which the neural network can pick up on. In contrast, feature selection and inference are more useful when the statistical problem is harder either because of limited data or weak signals, and neural networks or other black-box methods no longer have a clear advantage over simpler and more interpretable models.

D. Visualizing the results of the knockoffs filtering procedure

Fig. 2a shows an example of a raw Raman signal — we will denote it $X^{(1)}$. From this, we extracted wavelet features $X'^{(1)}$, from which the knockoffs procedure generates knockoff wavelet features $\tilde{X}'^{(1)}$. We can project this representation back into the signal domain using an Inverse Discrete Wavelet Transform. Fig. 2b shows the output of this operation. We observe that the while the ‘knockoff’ signal preserves characteristics of the original signal, such as is general shape and noise, it is identifiably distinct.

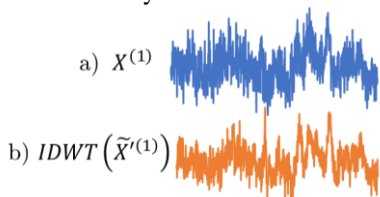


Fig. 2. (a) Sample raw Raman signal, $X^{(1)}$, and (b) the knockoff copy of the wavelet representation of the same sample, projected back into the signal domain, $IDWT(\tilde{X}'^{(1)})$.

We can also plot the correlations between the original features (Fig. 3a), as well as the cross-correlations between the original and knockoff wavelet features (Fig. 3b). The first 100 features or so, corresponding to the lower level DWT coefficients, show the highest local (adjacent feature) cross-correlations as seen in the insets; most of the other features are approximately uncorrelated. The cross-correlation maps in Fig. 3 should be consistent with Eq. (1), so Fig. 3b should look very similar to Fig. 3a, but with the values on its diagonal suppressed. This diagonal suppression is indeed what we observe for the most part, with the exception of the features in the original dataset with the strongest local cross-correlations. While the feature distribution may not be exactly multivariate Gaussian, our classification results indicate that the second-order knockoffs are effective in performing controlled feature selection, while retaining power in the selected features. Improvements in feature selection may be possible by using the deep knockoffs procedure [24] instead to capture the underlying feature distribution more accurately.

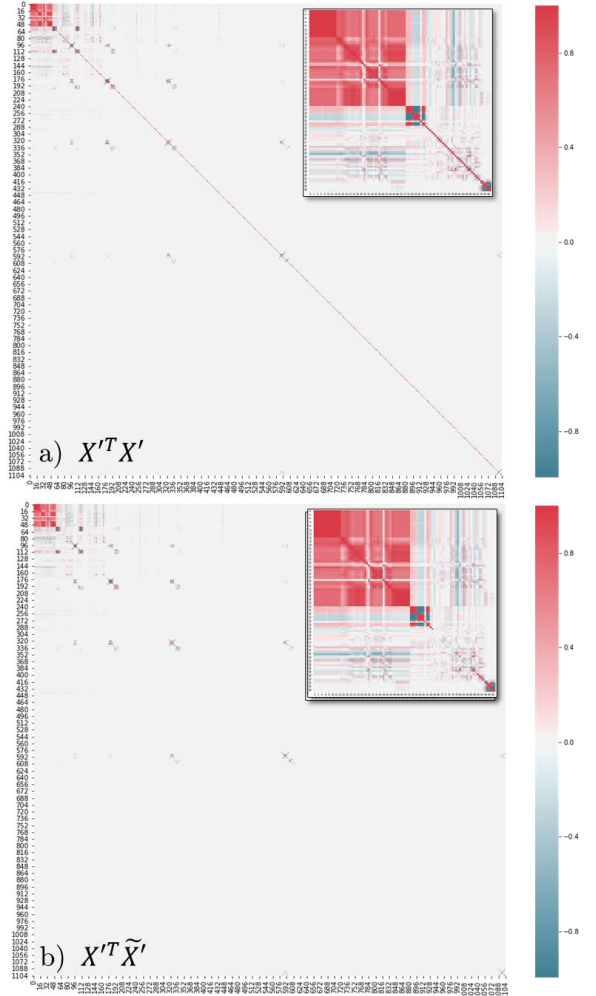


Fig. 3. Correlation map for (a) original wavelet features ($X'^T X'$); (b) original and knockoff wavelet features ($X'^T \tilde{X}'$). Inset: Zoomed in portion of map highlighting the first 100 features.

Finally, we can visualize the knockoff-filtered feature set in both the wavelet domain and signal domain, as seen in Fig. 4. The filtered signal was obtained by performing an inverse wavelet transform on the knockoff-selected wavelet features. These wavelets are mostly at lower frequencies; as might be expected, most of the high frequency wavelets are filtered out. Projecting them onto the signal domain, we see that much of the signal noise is removed and certain peaks are accentuated. In this way, features selected from a meaningfully chosen representation could reveal structures in the data important for the prediction task, in a way that the raw signal does not. In the case of our bacterial Raman dataset, selected wavelet-based peaks could correspond to distinguishing chemical signatures between different classes of bacteria. For various modalities of signal data, this knockoff-based framework for signal analysis could aid in model interpretation, allowing researchers to evaluate different morphologies of feature representations and achieve improved predictive accuracy and relevancy through controlled feature selection.

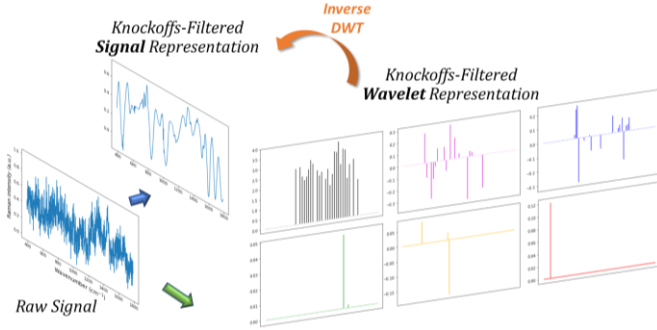


Fig. 4. Wavelet and Signal representations of features selected by Knockoff Filter

V. CONCLUSION

We have developed a general framework for applying the knockoffs filter method to signal data and demonstrated its efficacy on a dataset of Raman spectra from bacterial samples. Aimed at improving model interpretability as given by the PDR criterion, the framework first implements a transformation of the original features to a meaningful feature representation, then performs feature selection with FDR control, followed by model training. On the example dataset, we found that incorporating only transformed features also improves predictive accuracy, compared to the original full feature set. Our domain knowledge-based choice of the wavelet representation as well as a simple logistic regression-based classifier, resulted in predictive accuracy close to, and for certain tasks, better than, the CNN classifier reported in [27]. Other important advantages include a more compact model which was less computationally intensive to train, as well as superior descriptive accuracy and feature relevancy. At the same time, the flexibility and general nature of the framework offer the possibility of using different classifiers, as well as automating the feature engineering process. Overall, our framework provides a systematic and principled approach to the analysis of signal data, aiding in the development of human interpretable models with enhanced predictive performance.

Future work could explore the use of generative feature extraction models like DeepPINK or more complex and non-linear classifiers like neural networks, accompanied by an appropriate quantitative measure for feature importance, such as SHAP values. Alternative knockoff generation algorithms such as deep knockoffs could also enhance feature selection and improve the predictive accuracy of the framework. Finally, it would be interesting to investigate the impact of the nominal FDR level on the predictive accuracy of our method. In this paper, we have focused on the standard level of 10% for simplicity, and because larger values did not seem to bring much improvement. However, the optimal choice may generally depend on the details of the problem at hand.

APPENDIX

A. Overview of the knockoff filter method

The following provides an overview of the knockoff framework developed in [12]. Formally, we assume that there are n independent observations, and that the conditional distribution of observation $Y^{(i)}$ depends only on its corresponding vector of features $(X_1^{(i)}, \dots, X_p^{(i)})$ where $i = 1, \dots, n$, and p is the number of features in the input dataset. In summary, we have:

$$Y^{(i)} | (X_1^{(i)}, \dots, X_p^{(i)}) \sim F_{Y|X} \quad (\text{A1})$$

for some conditional distribution $F_{Y|X}$. The problem of feature selection is then that of finding the subset of *relevant* features $S \subset \{1, \dots, p\}$ upon which $F_{Y|X}$ actually depends. That is, conditional on $\{X_j\}_{j \in S}$, Y should be independent of all other features, which are termed *null*. We denote the subset of null features by H_0 . For a selection rule that selects a subset \hat{S} of the predictors, the false discovery rate (FDR) is defined as the expected fraction of false discoveries among all discoveries:

$$\text{FDR} = E \left[\frac{|\hat{S} \cap H_0|}{\max(1, |\hat{S}|)} \right] \quad (\text{A2})$$

The goal of the Knockoff Filter is to discover as many relevant features as possible while keeping the FDR under a specified level. It achieves this by manufacturing knockoff features that are cheap — their construction does not require collecting any new data — and are designed to mimic the dependency structure found within the original explanatory variables [8,10]. In particular, knockoffs must satisfy the following two conditions:

$$\text{i. } Y \text{ is independent of } \tilde{X} \mid X, \quad (\text{A3a})$$

$$\text{ii. } [X, \tilde{X}] \text{ and } [X, \tilde{X}]_{\text{swap}(S)} \text{ have the same distribution, for any subset } S \text{ of the features.} \quad (\text{A3b})$$

The first condition above states that knockoffs are null (this is easily achieved by generating them without looking at Y). The second condition states that the features in X and \tilde{X} are **pairwise exchangeable**, which implies that null features have equal explanatory power for Y as their corresponding knockoffs (in the sense explained below), and can thus properly serve as negative controls [12]. This equality in distribution is generally difficult to enforce exactly, so we make

some approximation and only match the first two moments, following in the footsteps of the previous literature [12,24].

The knockoff filtering procedure is implemented by first running a classifier on the *augmented feature set* $[X \tilde{X}]$. For each $j = 1, \dots, p$, we would then obtain scores Z_j and \tilde{Z}_j from the classifier output, that measure the importance of X_j and \tilde{X}_j in predicting Y . For instance, if we used a simple logistic regression with lasso regularization as the classifier, the scores could be given by $Z_j = |\hat{\beta}_j(\lambda)|$ and $\tilde{Z}_j = |\hat{\beta}_{j+p}(\lambda)|$, where $\hat{\beta}$ denotes the fitted coefficient matrix for the augmented feature set, and λ is the regularization parameter tuned by cross-validation. Ideally, we would like null features to have Z_j close to zero, although this may not generally be the case in practice; hence the need for knockoffs. We then compare the pairs of scores by combining them in a statistic W_j , using an anti-symmetric function $W_j = h(Z_j, \tilde{Z}_j)$, such as $W_j = Z_j - \tilde{Z}_j$. $W_j > 0$ would indicate that X_j appears to be more important than its knockoff copy, and is evidence against the null hypothesis $j \in H_0$. By construction of the knockoffs, the statistic W_j for *null* features has equal probability of being positive or negative; that is, the signs of null W_j 's are independent and identically distributed random coin flips [11].

We apply the Knockoff Filter by selecting only features that are clearly better than their knockoff copies. That is, we choose a feature j only if $W_j \geq t$, where t is an adaptive significance threshold. Fig. A1 illustrates this thresholding via the shaded region along the ordered sequence of $|W_j|$'s. The features corresponding to *positive* and shaded $|W_j|$'s are the ones selected.

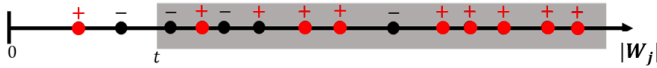


Fig. A1. Ordering of W_j 's by their absolute values

On the other hand, features with $W_j \leq -t$, corresponding to *negative* and shaded $|W_j|$'s, allow one to calculate a conservative estimate of the proportion of false discoveries $\widehat{FDP}(t)$ within the threshold [11]. In particular, FDR control can be provably achieved [11] by setting $t = T$ to be the smallest possible value such that $\widehat{FDP}(t) \leq q$, where q is the target FDR level, that is,

$$T = \min \left\{ t : \widehat{FDP}(t) = \frac{1 + \#\{j: W_j \leq -t\}}{\#\{j: W_j > t\}} \leq q \right\} \quad (\text{A4})$$

ACKNOWLEDGMENT

The authors would like to thank the Dionne group and its collaborators in the Ermon group at Stanford for their work on the collection and analysis of the Raman bacterial dataset used in this paper. Much thanks is also owed to Yaniv Romano in Candès group for his valuable input on the problem addressed in the paper. M. S. and E. C. are supported by NSF grant DMS 1712800. E. C. is also supported by a Math+X grant (Simons Foundation) and by NSF grant 1934578. C.-S.H, S.S.J., and J.A.D. acknowledge funding from the Stanford School of Engineering's Catalyst for Collaborative Solutions.

REFERENCES

- [1] L. H. Gilpin, D. Bau, B. Z. Yuan, A. Bajwa, M. Specter and L. Kagal, "Explaining Explanations: An Overview of Interpretability of Machine Learning," *2018 IEEE 5th International Conference on Data Science and Advanced Analytics (DSAA)*, Turin, 2018, pp. 80-89.
- [2] J. Murdoch, C. Singh, K. Kumbier, R. Abbasi-Asl and B. Yu, "Definitions, methods, and applications in interpretable machine learning," *Proceedings of the National Academy of Sciences*, vol. 116, no. 44, pp. 22071-22080, 2019.
- [3] Interpretable machine learning: A guide for making black box models explainable," C. Molnar, 2019. [Online]. Available: <https://christophm.github.io/interpretable-ml-book/>. Accessed on: Jan 7, 2020.
- [4] S. Krishnan and Y. Athavale, "Trends in biomedical signal feature extraction," *Biomedical Signal Processing and Control*, vol. 43, pp. 41-63, 2018.
- [5] Y. Bengio, R. Ducharme, P. Vincent and C. Jauvin, "A neural probabilistic language model," *Journal of Machine Learning Research*, vol. 3, pp. 1137-1155, 2003.
- [6] C. Farabet, C. Couprie, L. Najman and Y. LeCun, "Learning hierarchical features for scene labeling," *IEEE Transactions on Pattern Analysis and Machine Intelligence*, vol. 35, no. 8, pp. 1915-1929, 2013.
- [7] A. Borji, "Saliency Prediction in the Deep Learning Era: Successes, Limitations, and Future Challenges," *IEEE Transactions on Pattern Analysis and Machine Intelligence*, p. DOI: 10.1109/TPAMI.2019.2935715, 2019.
- [8] S. M. Lundberg and S.-I. Lee, "A Unified Approach to Interpreting Model Predictions," in *31st Conference on Neural Information Processing Systems*, Long Beach, 2017.
- [9] T. Miller, "Explanation in artificial intelligence: Insights from the social sciences," *Artificial Intelligence*, vol. 267, pp. 1-38, 2019.
- [10] S. Shete and R. Shriram, "Statistical Feature based Activity Classification," *International Journal of Computer Applications*, vol. 96, no. 15, pp. 49-51, 2014.
- [11] R. F. Barber and E. Candès, "Controlling the false discovery rate via knockoffs," *Annals of Statistics*, vol. 43, no. 5, pp. 2055-2085, 2015.
- [12] E. Candès, Y. Fan, L. Janson, and J. Lv, "Panning for Gold: 'Model-X' Knockoffs for High-dimensional Controlled Variable Selection", *Stat. Soc. B*, vol. 80, no. 3, pp. 551-577 (2018).
- [13] M. Sesia, E. Katsevich, S. Bates, E. Candès, C. Sabatti, "Multi-resolution localization of causal variants across the genome," *Nature Comm.*, vol. 11, no. 1093 (2020).
- [14] M. Sesia, C. Sabatti, and E. Candès, "Gene Hunting with Knockoffs for Hidden Markov Models," *Biometrika*, vol. 106, no. 1, pp. 1-18 (2019).
- [15] E. Katsevich, C. Sabatti, "Multilayer Knockoff Filter: Controlled variable selection at multiple resolutions," *Ann. Appl. Stat.*, vol. 13, no. 1, pp. 1-33, 2019.
- [16] A. Shen, H. Fu, K. He, H. Jiang, "False Discovery Rate Control in Cancer Biomarker Selection Using Knockoffs," *Cancers*, vol. 11, no. 6, pp. 744 (2019).
- [17] J. R. Gimenez, A. Ghorbani, and J. Zou, "Knockoffs for the mass: new feature importance statistics with false discovery guarantees," in *22nd International Conference on Artificial Intelligence and Statistics*, Okinawa, 2019.
- [18] X. Li, X. Dong, J. Lian, Y. Zhang, and J. Yu, "Knockoff filter-based feature selection for discrimination of non-small cell lung cancer in CT image," *IET Image Processing*, vol. 13, no. 3, pp. 543, 2019.
- [19] T. Nguyen, J. Chevalier, and B. Thirion, "ECKO: Ensemble of Clustered Knockoffs for Robust Multivariate Inference on fMRI Data," in *International Conference on Information Processing in Medical Imaging*, pp. 454-466, Hong Kong, 2019.
- [20] Y. Fan, J. Lv, M. Sharifvaghefi, and Y. Uematsu, "IPAD: Stable Interpretable Forecasting with Knockoffs Inference," *Journal of the American Statistical Association*, 2019.
- [21] C.-S. Ho, N. Jean, C. A. Hogan, L. Blackmon, S. S. Jeffrey, M. Holodniy, N. Banaei, A. A. E. Saleh, S. Ermon and J. Dionne, "Rapid identification of pathogenic bacteria using Raman spectroscopy and deep learning," *Nature Communications*, vol. 10, pp. 4927, 2019.

- [22] S. Mallat, *A Wavelet Tour of Signal Processing*, San Diego: Academic Press, 1999.
- [23] C. Garcia-Cardona and B. Wohlberg, "Convolutional Dictionary Learning: A Comparative Review and New Algorithms," *IEEE Transactions on Computational Imaging*, vol. 4, no. 3, pp. 366-381, 2018.
- [24] Y. Romano, M. Sesia and E. Candès, "Deep Knockoffs," *Journal of the American Statistical Association*, 2019.
- [25] G. Tutz, W. Pöbnecker and L. Uhlmann, "Variable Selection in General Multinomial Logit Models," University of Munich, Munich, 2012.
- [26] J. Friedman, T. Hastie, R. Tibshirani, B. Narasimhan, N. Simon and J. Qian, "glmnet: Lasso and Elastic-Net Regularized Generalized Linear Models," Stanford University, 15 11 2019. [Online]. Available: <https://cran.r-project.org/web/packages/glmnet/index.html>.
- [27] C.-S. Ho, N. Jean, C. A. Hogan, L. Blackmon, S. S. Jeffrey, M. Holodniy, N. Banaei, A. A. E. Saleh, S. Ermon and J. Dionne, "Rapid identification of pathogenic bacteria using Raman spectroscopy and deep learning," *arXiv:1901.07666*, 2019.